Supercritical CO_2-Assisted Synthesis of Polystyrene/Clay Nanocomposites via in situ Intercalative Polymerization

Jianbo Li, Qun Xu, Qi Peng, Maizhi Pang, Suqin He, Chengshen Zhu

College of Materials Engineering, Zhengzhou University, Zhengzhou, China

Received 28 February 2005; accepted 19 July 2005
DOI 10.1002/app.23395
Published online in Wiley InterScience (www.interscience.wiley.com).

ABSTRACT: Na-montmorillonite was modified by cetyltrimethylammonium bromide (CTAB) to enlarge the distance between the two silicate layers and to improve these silicate layers' organophilicity. The organic intercalation reagent had intercalated into the galleries of montmorillonite as determined by FTIR and wide angle X-ray diffraction (WAXD). Then, polystyrene (PS)/clay nanocomposites (PSCN) were successfully prepared by means of in situ intercalative polymerization using supercritical carbon dioxide (SC CO_2) as monomer/initiator carrier. During the process, both SC CO_2/montmorillonite binary system and SC CO_2/monomer/montmorillonite ternary system were studied. Exfoliated and intercalated PSCN can be obtained, respectively, by adjusting the content of clay in PS matrix, which was confirmed by WAXD and by transmission electron microscopy (TEM). Thermal analysis performed with thermal gravimetric analysis (TGA) and differential scanning calorimetry (DSC) indicates PSCN has superior thermal stability to pristine PS. © 2006 Wiley Periodicals, Inc. J Appl Polym Sci 100: 671–676, 2006

Key words: supercritical CO_2; nanocomposite; in situ polymerization; thermal property

INTRODUCTION

Inorganic–organic composites have been widely investigated because of their potential applications in many fields, such as mechanics, electronics, coatings, and automobiles. These composites inherit some of the properties of both organic and inorganic materials.[1–3] Among these composites, polymer/clay nanocomposites have attracted great attention[4–6] because of their unusual properties, such as improved modulus,[7] decreased thermal expansion coefficient,[8,9] reduced gas permeability,[10] and enhanced ionic conductivity.[11] Several attempts to prepare polymer/clay nanocomposites have been reported.[12,13] Typical preparation methods include in situ polymerization, solution intercalation, and melt intercalation. The in situ polymerization is well-known to provide in a simple way that involves intercalating monomer and initiator in clay followed by polymerization. The clay that is most generally used is montmorillonite (MMT), and an important step for producing these nanocomposites is to render these MMT layers organophilic by ion exchange reactions.

During the past decade, supercritical fluids (SCFs), due to their low viscosity, high diffusivity, zero surface tension, and strong solvent power for many organic compounds, have been applied in the synthesis of composites. For example, these unique properties of SC CO_2 have been exploited to prepare polymer blend.[14–20] Recently, polystyrene (PS) has been encapsulated into the hollow CNTs with the aid of SC CO_2, and the filling fraction can be controlled by the speed at which the CO_2 is released during the soaking process.[21]

Intercalation of unreactive small molecules into layered clay in the presence of SC CO_2 has also been described.[22,23] Recently, Samulski et al. have successfully intercalated poly(ethylene oxide) into layered MMT clay via a CO_2-mediated process, but they use SC CO_2 as a plasticization medium, but not solvent.[24] In Lesser's recent report, an in situ polymerization method used SC CO_2 as a processing aid to achieve a uniform reinforcement distribution in a polymer/clay composite at high clay loading(~40 wt %).[25] SC CO_2 is used to homogeneously distribute monomer as well as act as a low-viscosity solvent for methyl methacrylate (MMA) polymerization.

In this article, we present a modified synthetic route to produce polymer/clay nanocomposite where styrene monomer and initiator were directly intercalted into organomontmorillonite (OMMT) with the aid of SC CO_2, followed by depressurization and free-radical

Correspondence to: Q. Xu (qunxu@zzu.edu.cn).
Contract grant sponsor: National Natural Science Foundation of China; contract grant number: 20404012.
Contract grant sponsor: Prominent Youth Science Foundation of Henan Province; contract grant number: 0512001200.
Contract grant sponsor: Henan Natural Science Foundation; contract grant number: 0411020900.

polymerization. The polystyrene/clay nanocomposites (PSCN), with intercalated or exfoliated structure, can be obtained by in situ polymerization, which was confirmed by WAXD and TEM. Our purpose is to systematically investigate the effects of SC CO_2 on the intercalation of monomer, the structure and thermal properties of the nanocomposites.

EXPERIMENTAL

Materials

The Na-montmorillonite(MMT) used in this experiment was supplied by the Institute of Chemical Metallurgy, Chinese Academy of Sciences. MMT is a natural clay mineral with a cation exchange capacity of 100 meq/100 g. Cetyltrimethylammonium bromide (CTAB) was purchased from Tianning Chemical Reagent Co.(Jining, China). CO_2 with purity of 99.9% was obtained from Zhengzhou Sanfa Gas Co. (Zhengzhou, China). Styrene was purchased from Tianjin Jinyu Chemical Plant (Tianjin, China) and distilled under reduced pressure. Azobis (isobutyronitrile) (AIBN) supplied by Shanghai Sanpu Chemical Co. (Shanghai, China) was recrystallized twice from methanol.

Procedures

Reactions were run in a 50-mL high-pressure stainless steel reactor equipped with sapphire window that allows visual observation. A high-pressure syringe pump (Beijing Satellite Manufacturing Factory, Beijing, China; DB-80) was used to charge CO_2 into the reaction vessel and attached to the reactor via a coupling and high-pressure tubing. A pressure gauge consisting of a transducer (IC Sensors Co., Model-93) and an indicator (Beijing Tianchen Automatic Instrument Factory, XS/A-1) with the accuracy of ± 0.05 MPa was also connected to the reactor to observe the in situ pressure change of the system. In the experiments, the reactor was placed in a constant-temperature circulator, which consisted of a temperature control module (Thermo Haake, C10) and a bath vessel (Thermo Haake, P5). The fluctuation of temperature in the bath was less than ± 0.1°C. All samples were weighed on a Shanghai 328A electrobalance with a sensitivity of 0.1 mg.

Preparation of OMMT material

CTAB of 15 g was dispersed in 300-mL warm distilled water, and the solution was blended with 1000-mL suspension of layered clay. The mixture was stirred at 65°C for 3 h. Then, it was washed and filtrated under vacuum, and the sediments were dried under vacuum at 100°C for 10 h. The dried sediment was denominated OMMT.

Study of the compatibility between the styrene and SC CO_2

To determine the compatibility between the styrene and SC CO_2, a known amount of styrene was charged into the visual-window high-pressure cell. To remove the air out off the cell, it has been purged twice by gaseous CO_2 at condition ambient. Then, the reactor was equilibrated in water bath of 40°C and pressurized to the desired pressure. When the pressure has been reached and the mixture was homogenized by stirring, pressure would slowly decrease again, until a second phase appeared at the dew point. This process was repeated until the separation pressure was reproduced in a small pressure range. Then, different swelling ratio of the solution in SC CO_2 was obtained at different pressures.

Study of SC CO_2/OMMT binary system

A certain amount of OMMT powder was weighed into a small cuvette, which was put in the high-pressure reactor. After being purged with CO_2 twice and equilibrated in the constant-temperature bath, the reactor was repressurized to the desired pressure. After a period of soaking, the reactor was depressurized and the samples were brought to an electronic balance immediately. Then, the treated samples were placed in 25°C, clean and dry atmosphere for 12 h, and mass change was recorded regularly.

Study of SC CO_2/monomer/OMMT ternary system

Initiator AIBN of 0.3 mol % (based on styrene) was dissolved in 3 mL of styrene, and then the solution was placed in the bottom of the reactor. Then, some glass wool was put in, upon which the small cuvette containing a suitable amount of dried OMMT powder were placed. So, before charging CO_2 into the reactor, samples and monomer solution did not touch each other. After being purged with CO_2 twice, the reactor was equilibrated in a 40°C water bath and repressurized to the desired pressure. After a period of soaking, the reactor was depressurized. The small cuvette was brought out and weighed, and mass change was recorded regularly.

Synthesis of PS/clay nanocomposites

A desired amount of dried OMMT powder was mixed with styrene and 0.3 mol % (based on styrene) initiator AIBN solution in a glass vial, and then placed into a 50-mL stainless steel vessel. After magnetically stirring for about 30 min, the air in the vessel was re-

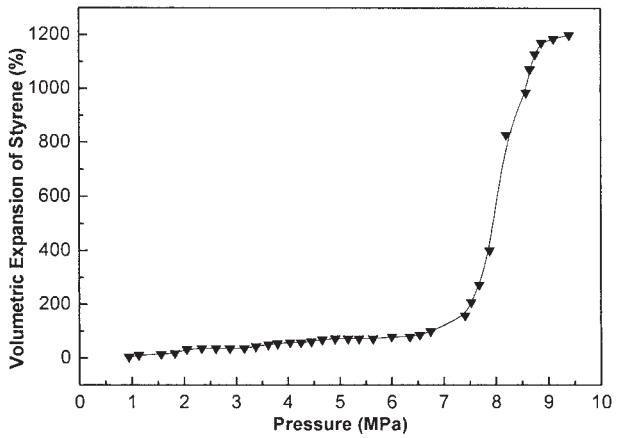

Figure 1 Volumetric expansion of styrene (0.52 mol/L) with compressed CO_2 as a function of pressure at 313 K.

moved by blowing CO_2 at ambient condition. The vessel was then put into a water bath of 40°C, the vigorous magnetically stirring was turned on, and CO_2 was introduced to the desired pressure by a high-pressure syringe pump. After soaking for 4 h, CO_2 was released, and then the vessel was transferred into an oven at 70°C to initiate the polymerization of styrene. After reacting for 12 h, the vessel was cooled to room temperature. The resultant composites were dried under vacuum.

Characterization

Infrared (IR) spectroscopy experiments were performed using a Nicolet 460 FTIR under standard operating conditions. Wide angle X-ray diffraction (WAXD) patterns were recorded by monitoring the diffraction angle 2θ from 1.4 to 20° on a Rigaku D/MAX-IIIB X-ray diffractometer using Cu Kα radiation (λ = 0.154 nm) operated at 35 kV and 30 mA. Differential scanning calorimetry (DSC) measurements were conducted on a Netzsch 204 DSC under N_2 atmosphere with a heating rate of 10°C/min in the temperature range of 30–120°C. Thermogravimetric analysis (TGA) was performed using a Netzsch TG209 instrument with a heating rate of 10°C/min and a heating range from 30°C to 550°C under N_2 atmosphere. Transmission electron micrographs (TEM) were obtained with a JEM-100SX using an acceleration voltage of 80 kV. The sample is obtained by routine freezing ultrathin sampling.

RESULTS AND DISCUSSION

Compatibility between the styrene and SC CO_2

The compatibility between the styrene and SC CO_2 was studied by the swelling of styrene in SC CO_2. Larger the swelling of the solution in SC CO_2, the stronger is the compatibility between the styrene and SC CO_2. The experimental results are shown in Figure 1. The volume expansion of styrene in SC CO_2 was denoted $\Delta V\%$, which is given in eq. (1).

$$\Delta V\% = [V(P,T) - V(P_0,T)]/V(P_0,T) \times 100\% \quad (1)$$

where P_0 represents the atmospheric pressure, T is the temperature of the system. From Figure 1, we could see that the compatibility of styrene and SC CO_2 was perfect above 9 MPa, i.e., SC CO_2 could be used as carrier for styrene intercalating clay.

Sorpotion and desorpotion of CO_2 and styrene in pristine OMMT

The sorption and desorption kinetics of CO_2/OMMT system were measured using a method similar to that described by Berens and Huvard.[26,27] Through these measurements, average mass gain was calculated, and the results were plotted versus the square root of desorption time. In Figure 2, the plots appear linear versus the square root of time and within the experimental error range, this demonstrates that the desorption kinetics of unreactive small molecules in OMMT conforms to Fickian's Diffusion Kinetics.

In addition to uptake of CO_2 by the substrate, uptake of styrene by OMMT at same condition was also determined. In Figure 3, it is found that the desorpotion kinetics of CO_2 in the presence of styrene are similar to those without styrene. When samples were weighed immediately after being treated, the difference of mass gain between them was 22.05 g/100 g OMMT. After 6600 s, the difference was 21.50 g/100 g OMMT, almost unchanged. This demonstrates that with releasing CO_2, mass loss of the incorporated

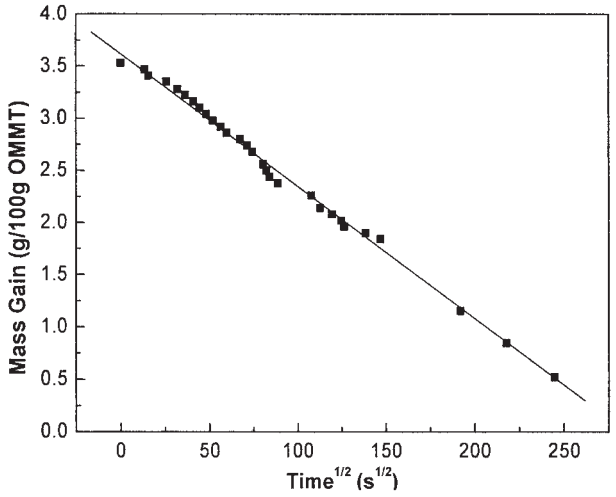

Figure 2 Mass gain of OMMT as a function of the square root of desorption time after being treated in SC CO_2 for 4 h at 40°C and 12 MPa.

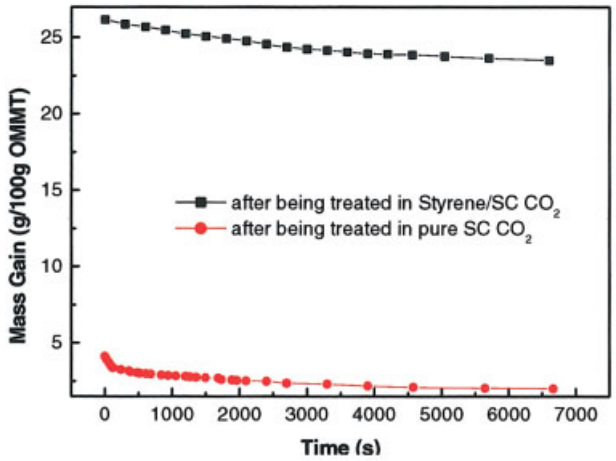

Figure 3 Mass gain of OMMT as a function of desorption time after being treated in SC CO_2 and in styrene/SC CO_2 for 4 h at 40°C and 12 MPa. [Color figure can be viewed in the online issue, which is available at www.interscience.wiley.com.]

styrene is little and an absolute majority remained in the substrate.

IR spectra

Figure 4 shows the FTIR spectra of the pristine Na-MMT, OMMT, PSCN, and pristine PS. The characteristic vibration peaks of Na-MMT [Fig. 4(a)] and OMMT [Fig. 4(b)] both appear at 3629 cm^{-1}(O—H stretching), 1039 cm^{-1} and 1094 cm^{-1} (Si—O stretching), 466–624 cm^{-1} (Al—O and Si—O bending). But for OMMT, there are two obvious new absorption peaks, which appear at 2851 and 2920 cm^{-1} (C—H asymmetric and symmetric stretching) in Figure 4(b). And, this demonstrates that the organic intercalation reagent (CTAB) has already been exchanged into the galleries of MMT.

In Figure 4(d), we can see that the characteristic vibration peaks of PS appear at 1452, 1493, and 1601 cm^{-1} (aromatic C—C stretching), 696 and 756 cm^{-1} (aromatic C—H bending), 3000–3100 cm^{-1}(aromatic C—H stretching). Besides those of PS, the IR spectra of PSCN [Fig. 4(c)] also have the characteristic vibration peaks of OMMT, which are shown in Figure 4(b). The OMMT content is very little (only 5 wt %) in PS/clay nanocomposite sample, which was adopt in IR characterization. This suggests that the layered silicates have already been dispersed into the polystyrene hosts evenly.

XRD

The XRD patterns show the spacing changes of clay gallery (d_{001}) according to Bragg diffraction eq. (2)

$$2d \sin\theta = \lambda \quad (2)$$

where, d represents the average interlayer spacing of the silicates, θ is 1/2 of the diffraction angle, λ is the wavelength of the incident X-ray (λ = 1.5416Å).

XRD patterns of the pristine Na-MMT and OMMT are shown in parts (a) and (b) of Figure 5, respectively. After the ion-exchange treatment, shift of the clay diffraction peaks suggest the increase of the clay galleries, for some bulky organic cations replacing the Na^+ exchange cations of the native clay. The peak (001) of the OMMT shifts from 1.29 nm in the pristine Na-MMT to 2.06 nm. This is another successful evidence that the organic intercalation reagent (CTAB) has already been exchanged into the galleries of MMT.

The XRD patterns of a series of PSCN samples with different OMMT content are shown in parts (c)–(e) of Figure 5. There is a lack of diffraction peak at 2θ = 1.4–10° for PSCN sample with 3.0% OMMT, as opposed to the diffraction peak at 2θ = 4.28° (d spacing = 2.06 nm) for pristine OMMT, indicating the possibility of exfoliated silicate nanolayers of OMMT

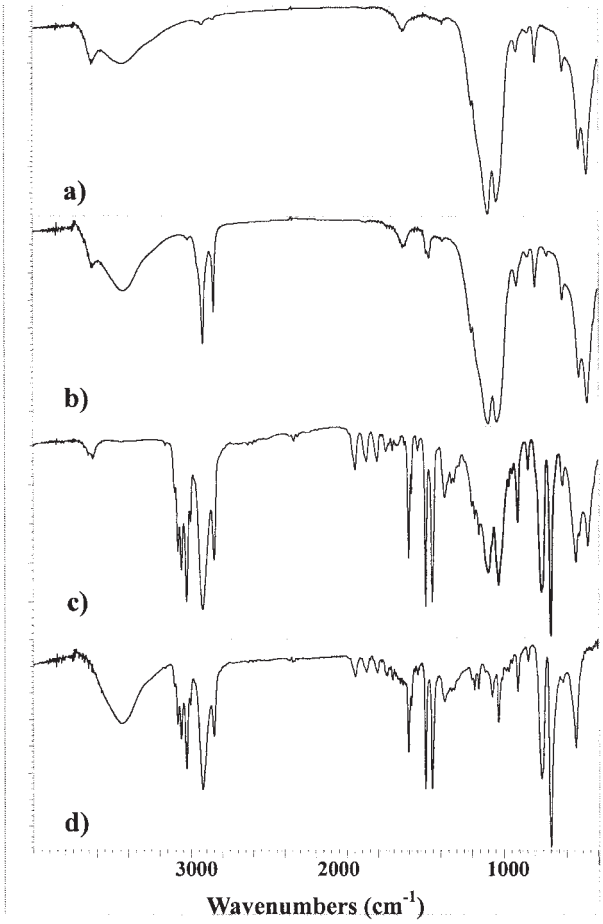

Figure 4 FTIR spectra of the samples: (a) pristine Na-MMT; (b) OMMT; (c) PSCN (OMMT content: 5.0%); and (d) pristine PS.

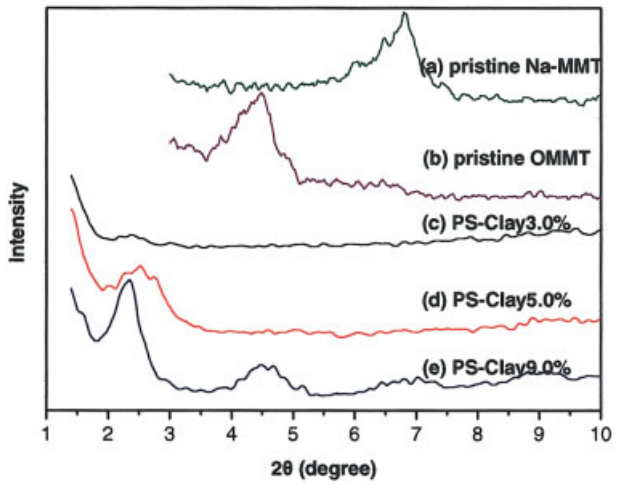

Figure 5 XRD patterns of the pristine Na-MMT, OMMT, and a series of PSCN materials. [Color figure can be viewed in the online issue, which is available at www.interscience.wiley.com.]

dispersed in the PS matrix. When the amount of OMMT increases to 5.0%, small peaks appear at $2\theta = 2.52°$, corresponding a d spacing of 3.50 nm. This implies that there is a small amount of OMMT that cannot be exfoliated in the PS and exists in the form of an intercalated layer structure. When OMMT content is up to 9.0%, a new smaller peak appears at $2\theta = 4.28°$, which is just correspondent to the diffraction peak of pristine OMMT, as suggests that the OMMT content have already been excessive at this moment. Then, we can deduce that a series of PSCN materials with different nanomorphology can be got, respectively, through adjusting the OMMT content.

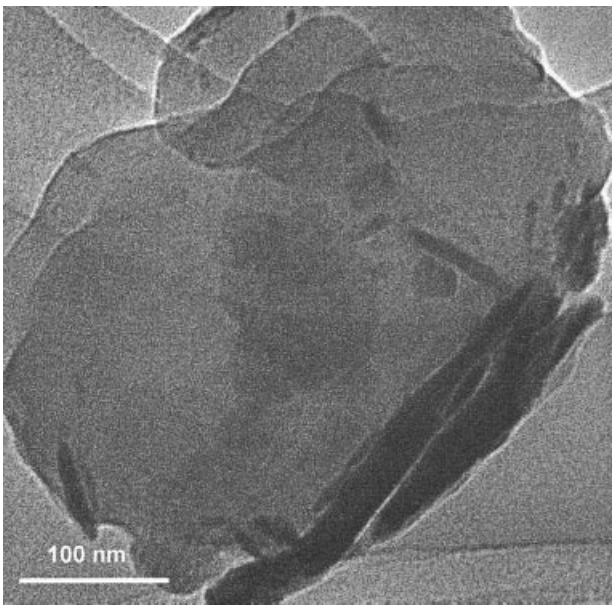

Figure 6 TEM of PSCN material with 3.0% clay loading.

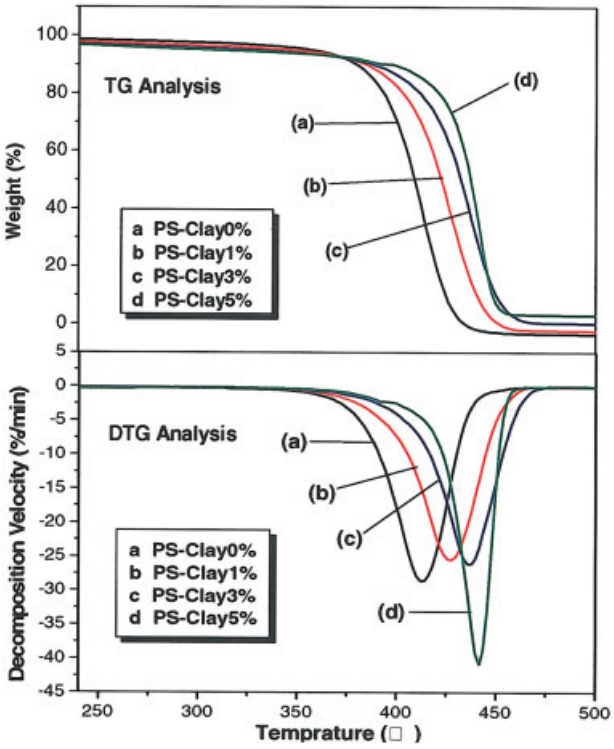

Figure 7 TG and DTG curves of PS and a series of PSCN materials. [Color figure can be viewed in the online issue, which is available at www.interscience.wiley.com.]

TEM

The dispersion microstructure of the intercalated silicate layers was also examined by means of TEM. In Figure 6, the TEM of PSCN material with 3.0% clay loading reveals that the nanocomposite displays a mixed nanomorphology. Individual silicate layers,

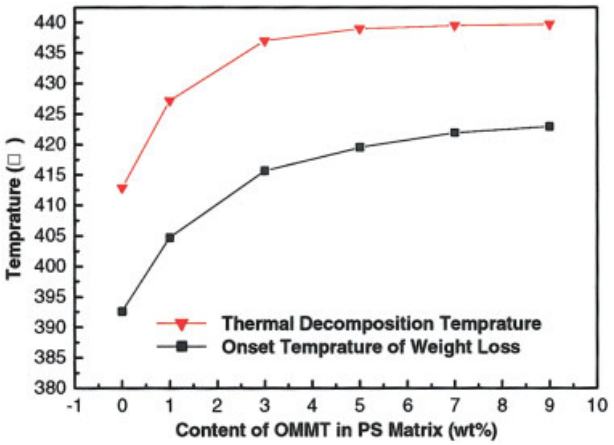

Figure 8 Thermal decomposition temperature and onset temperature of weight loss of PS and a series of PSCN materials as a function of OMMT content in PS matrix. [Color figure can be viewed in the online issue, which is available at www.interscience.wiley.com.]

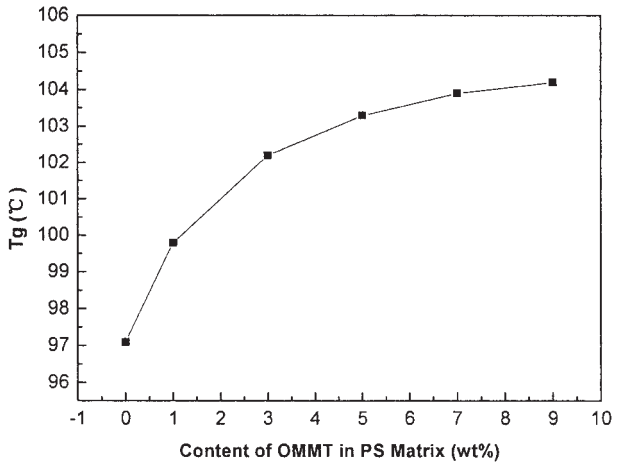

Figure 9 Glass-transition temperature (T_g) of PS and a series of PSCN materials as a function of OMMT content in PS matrix.

along with two and three layer stacks, are found to be exfoliated in the PS matrix. In addition, some larger intercalated tactoids can also be identified.

TGA and DSC analysis

Figure 7 shows typical TGA thermograms of weight loss as a function of temperature for the PS and a series of PSCN materials, as measured under an N_2 atmosphere. Evidently, the thermal decomposition of the PSCN materials shifts toward higher temperatures than that of PS, which confirms the enhancement of thermal stability of the clay-modified PS. The higher decomposition temperature is frequently attributed to the barrier characteristics of clay nanolayers, which induce a tortuous pathway for volatile degradation products, but there may be specific clay–PS interactions that also increase the thermal stability.[13,24] Meanwhile, we find that the thermal decomposition temperature of PS rises with the increasing of OMMT content. And, in Figure 8, we can see that when OMMT content is too high, the range that decomposition temperature increases will be smaller and smaller. This is in conformity with the results of preceding XRD analysis.

To obtain the further evidence, we have carried on DSC analysis to the pure PS and a series of PCN materials, and the results are shown in Figure 9. All of the PSCN materials show an increased glass-transition temperature (T_g) compared to that of pure PS is 97.1°C. This is tentatively attributed to the confinement of the intercalated polymer chains within the clay galleries that prevents the segmental motions of the polymer chains. And, the trend that T_g increase with the OMMT content is similar to thermal decomposition temperature.

CONCLUSIONS

A series of PSCN were prepared by means of SC CO_2-assisted in situ intercalative polymerization, in which SC CO_2 was used as monomer/initiator carrier. The nanomorphology of PSCN materials can be controlled by adjusting the OMMT content. Moreover, characterization shows that the prepared PSCN materials have much better thermal stability than native PS. This kind of method can be extended to the preparation of many other polymer/clay nanocomposites.

References

1. Wozniak, M. E.; Sen, A. Chem Mater 1992, 4, 754.
2. Novak, B. M. Adv Mater 1993, 5, 422.
3. Beecroft, L. L.; Ober, C. K. Chem Mater 1997, 9, 1302.
4. Usuki, A.; Kawasumi, M.; Kojima, Y.; Okada, A.; Kurauchi, T.; Kamigaito, O. J Mater Res 1993, 8, 1174.
5. Giannelis, E. P.; Krishnamoorti, R.; Manias, E. Adv Polym Sci 1999, 138, 107.
6. Biswas, M.; Ray, S. S. Adv Polym Sci 2001, 155, 167.
7. Maiti, P.; Yamada, K.; Okamoto, M.; Ueda, K.; Okamoto, K. Chem Mater 2002, 14, 4654.
8. Itagaki, T.; Komori, Y.; Sugahara, Y.; Kuroda, K. J Mater Chem 2001, 11, 3291.
9. Sun, T.; Garces, J. M. Adv Mater 2002, 14, 128.
10. Usuki, A.; Tukigase, A.; Kato, M. Polymer 2002, 43, 2185.
11. Kim, J. W.; Liu, F.; Choi, H. J.; Hong, S. H.; Joo, J. Polymer 2003, 44, 289.
12. Kim, T. H.; Lim, S. T.; Lee, C. H.; Choi, H. J.; Jhon, M. S. J Appl Polym Sci 2003, 87, 2106.
13. Kim, T. H.; Jang, L. W.; Lee, D. C.; Choi, H. J.; Jhon, M. S. Macromol Rapid Commun 2002, 23, 191.
14. Elkovitch, M. D.; Tomasko, D. L.; Lee, L. J. Polym Eng Sci 1999, 39, 2075.
15. Wang, J.; Cheng, X.; Zheng, X.; Yuan, M.; He, J. J Polym Sci Part B: Polym Phys 2003, 41, 368.
16. Hayes, H. J.; McCarthy, T. J. Macromolecules 1998, 31, 4813.
17. Arora, K. A.; Lesser, A. J.; McCarthy, T. J. Macromolecules 1999, 32, 2562.
18. Xu, Q.; Chang, Y.; He, J.; Han, B.; Liu, Y. Polymer 2003, 44, 5449.
19. Chang, Y.; Xu, Q.; Liu, M.; Wang, Y.; Zhao, Q. J Appl Polym Sci 2003, 90, 2040.
20. Chang, Y.; Xu, Q.; Han, B.; Wang, Y.; Liu, M.; Zhao, Q. J Appl Polym Sci 2004, 92, 2023.
21. Liu, Z.; Dai, X.; Xu, J.; Han, B.; Zhang, J.; Wang, Y.; Huang, Y.; Yang, G. Carbon 2004, 42, 458.
22. Shi, T. P.; Yao, K.; Nishimura, S.; Imai, Y.; Yamada, N.; Abe, E. Chem Lett 2002, 4, 440.
23. Yoda, S.; Sakurai, Y.; Endo, A.; Miyata, T.; Otake, K.; Yanagishita, H.; Tsuchiya, T. Chem Commum 2002, 14, 1526.
24. Zhao, Q.; Samulski, E. T. Macromolecules 2003, 36, 6967.
25. Zerda, A. S.; Caskey, T. C.; Lesser, A. J. Macromolecules 2003, 36, 1603.
26. Berens, A. R.; Huvard, G. S.; Kormeyer, R. W.; Kunig, F. W. J Appl Polym Sci 1992, 46, 231.
27. Berens, A. R.; Huvard, G. S. In Supercritical Fluid Science and Technology; Johnston, K. P., Penniger, J. M. L., Eds. ACS symposium series 406. American Chemical Society: Washington, DC, 1989.